Asian Transport Studies 6 (2020) 100007

Contents lists available at ScienceDirect

Asian Transport Studies

journal homepage: www.journals.elsevier.com/asian-transport-studies

Modeling joint activity-travel patterns in pedestrian networks with use of Wi-Fi data☆

Khoa D. Vo [a], Kun Qian [a], William H.K. Lam [a,*], Agachai Sumalee [b]

[a] Department of Civil and Environmental Engineering, The Hong Kong Polytechnic University, Hong Kong
[b] School of Integrated Innovation, Chulalongkorn University, Bangkok, Thailand

ARTICLE INFO

Keywords:
Activity-travel scheduling
Network equilibrium
Intragroup interactions
Pedestrian network

ABSTRACT

This paper proposes a new activity-based equilibrium model to solve a joint activity-travel pattern scheduling problem in pedestrian networks. A novel supernetwork platform, pedestrian-joint-activity-time-space, is proposed to capture the complex structure of pedestrian networks and intragroup interactions on joint activity choices of pedestrians. The joint activity-travel pattern scheduling problem is transformed into an extended static user equilibrium traffic assignment model with side constraints for group interactions. A heuristic solution method is proposed to solve the user equilibrium problem concerned. A simplified pedestrian network is used to illustrate the convergence of the proposed heuristic solution method. Furthermore, the use of Wi-Fi tracking data from mobile phones to generate the activity patterns of pedestrians and their interactions is also investigated with a real case study in a selected area of The Hong Kong Polytechnic University.

1. Introduction

Understanding and predicting pedestrian activity and travel demand play an important role in the efficient design of new infrastructure, such as facilities on university campuses or in shopping centers, and in the daily operations of such infrastructure. The spatiotemporal consistency of pedestrians' activity/travel choices and intragroup interactions of behaviorally heterogeneous group members requires explicit modeling of activity-travel scheduling decisions. These decisions can be classified into three levels: (1) departure time choice and activity pattern choice (*strategic level*); (2) activity scheduling and route/mode choice (*tactical level*); and (3) walking behavior (*operational level*) (Hoogendoorn and Bovy (2004)).

Although modeling pedestrian walking behaviors such as the choice of walking orientation and speed plays a central role in pedestrian behavior research (see Hoogendoorn et al. (2002) and Bierlaire and Robin (2009)), activity-travel choice models for pedestrians at the strategic and tactical levels have received little attention. Hoogendoorn and Bovy (2004) developed an activity-travel scheduling model in a continuous time-space pedestrian network, but their model focused mainly on the tactical level. Activity-travel scheduling models in pedestrian networks can be distinguished from existing counterpart models in transportation networks (e.g., Miller and Roorda (2003), Bhat et al. (2004), Arentze and Timmermans (2004), and Roorda et al. (2009)) in the following aspects. First, pedestrian networks have a more complex structure than transportation networks. In particular, pedestrian networks include various types of points at multiple levels (floors), such as pathways, stairways, escalators, and elevators. Second, the intragroup interactions of behaviorally heterogeneous pedestrians within the same group also play an important role in activity choice behavior. Finally, crowding effects at activity locations may affect pedestrians' activity choices.

Lam and Yin (2001) first proposed an activity-based equilibrium model in which a time-expanded supernetwork was used to capture individuals' spatiotemporally constrained activity-travel scheduling behavior. This model was followed by the use of activity-time-space (ATS) supernetworks, which are extended from the time-expanded supernetwork, for schedule-based transit systems (Li et al. (2010)), congested networks (Ouyang et al. (2011)), stochastic utilities (Fu and Lam (2014)), and weather effects (Fu et al. (2014)). Fu and Lam (2018) developed a joint-activity-time-space (JATS) supernetwork platform to model the joint activity and travel choices of two persons in multimodal

* Corresponding author.
E-mail addresses: khoa.v.dang@gmail.com (K.D. Vo), queenie.qian@connect.polyu.hk (K. Qian), william.lam@polyu.edu.hk (W.H.K. Lam), asumalee@gmail.com (A. Sumalee).

https://doi.org/10.1016/j.eastsj.2020.100007
Received 23 April 2020; Received in revised form 29 May 2020; Accepted 19 June 2020
Available online 6 August 2020

transit networks. The modeling of joint activities in their study, however, was simplified in that each individual's schedule contained a maximum of one joint activity. Vo et al. (2020) proposed a household utility optimum to model the joint activity and travel choices of private car users with more generalized interactions of various household types using different transportation modes (i.e., private car or public transit). Nevertheless, no studies have focused on modeling the activity and travel choices of pedestrians and their interactions.

In this paper, we propose a novel activity-based equilibrium model to schedule the daily joint activity-travel patterns (JATPs) of pedestrians, hypothesizing that behaviorally heterogeneous pedestrians in the same group may have joint activities and are affected by crowding discomfort while walking and participating in activities. We then propose a pedestrian-joint-activity-time-space (PJATS) supernetwork platform to capture the complex structure of pedestrian networks and interactions on the joint activities of pedestrians. Based on the proposed PJATS supernetwork, the JATPscheduling problem is transformed into an extended static user equilibrium (UE) assignment problem with additional constraints for intragroup interactions. A heuristic solution method, based on the method of successive averages (MSA), is proposed to address the extended UE problem. To generate the JATP choice set at each iteration of the solution method, a multi-agent path finding (MAPF) algorithm is adopted. Furthermore, the use of Wi-Fi tracking data from mobile phones is investigated and illustrated to generate an activity pattern for pedestrians and their joint activities within a selected study area on The Hong Kong Polytechnic University (PolyU) campus.

The rest of this paper is organized as follows. First, the model assumptions are given in Section 2, the network representation is proposed in Section 3, and the problem formulation and solution method are presented in Sections 4 and 5. The numerical example is given in Section 6, followed by an experimental study at PolyU with the use of Wi-Fi tracking data to generate the activity pattern of pedestrians and their joint activities. Finally, our conclusions are given in Section 7, with recommendations for further studies.

2. Model assumptions

To facilitate essential ideas without loss of generality, several assumptions have been adopted in this paper:

(1) JATPs are considered in a fixed study horizon divided into equally spaced time intervals (Lam and Yin (2001), Ouyang et al. (2011), and Fu et al. (2014)).
(2) Travel times in the pedestrian network are deterministic and flow-dependent (Lam and Yin (2001), Ouyang et al. (2011) and Fu et al. (2014))), and dynamic and stochastic walking behavior is not considered (Hoogendoorn and Bovy (2004)).
(3) Activity utilities and travel disutilities are deterministic and flow-dependent (Lam and Yin (2001), Ouyang et al. (2011), and Fu et al. (2014)).
(4) Pedestrians have perfect knowledge of traffic conditions throughout the network (Fu and Lam (2014)) and activity locations. Note that the proposed model is used mainly for long-term infrastructure planning and facility management purposes.
(5) The joint decision-making process seeks to maximize the utility of JATP of the entire group (Fu and Lam (2018), and Vo et al. (2020)).

Some abbreviations used in the paper are summarized as follows:

- PJATS: Pedestrian-Joint-Activity-Time-Space supernetwork
- JATP: Joint Activity-Travel Pattern
- ATP: Activity-Travel Pattern
- UE: User Equilibrium
- MSA: Method of Successive Averages
- MAPF: Multi-Agent Path Finding
- CBS: Conflict-Based Search
- DBSCAN: Density-Based Spatial Clustering of Applications with Noise
- HMM: Hidden Markov Model
- MAC address: Media Access Control address
- PolyU: The Hong Kong Polytechnic University

3. Network representation

3.1. Pedestrian-joint-activity-time-space (PJATS) supernetwork

Given a pedestrian network, a PJATS supernetwork $G^{ig}(N^{ig}, E^{ig})$ is constructed for each member i of group g, where N^{ig}, E^{ig} are the set of nodes and links, respectively. Each PJATS supernetwork G^{ig} captures both separate and joint activities of member i with other group members. The nodes and links of G^{ig} are composed of the exclusive subsets below.

- $N^{ig} = N^{ig}_{act} \cup N^{ig}_{loc} \cup N^{ig}_{start} \cup N^{ig}_{end}$,
- $E^{ig} = E^{ig}_{act} \cup E^{ig}_{wait} \cup E^{ig}_{travel} \cup E^{ig}_{exchange} \cup E^{ig}_{ingress} \cup E^{ig}_{egress} \cup E^{ig}_{start} \cup E^{ig}_{end}$,

where

- Node $(a, l, z, m \cup \{i\}, k) \in N^{ig}_{act}$, $m \subseteq g$, is an *activity node*. It represents a state in which a group of members m, including i, jointly participates in an activity a at time k at location l on floor z, or in short location (l, z).
- Node $(l, z, k) \in N^{ig}_{loc}$ is a *location node*. It represents a state in which member i stays at location (l, z) at time k.
- Node $Start(i) \in N^{ig}_{start}$ is a *start node*. It is a *dummy* start node for member i.
- Node $End(i) \in N^{ig}_{end}$ is an *end node*. It is a *dummy* end node for member i.
- Link $(a, l, z, m, k) \rightarrow (a, l, z, m, k+1) \in E^{ig}_{act}$, $m \subseteq g$, is an *activity link*. It represents that a group of members m, including i, performs activity a from time k to time $k+1$ at location (l, z).
- Link $(l, z, k) \rightarrow (l, z, k+1) \in E^{ig}_{wait}$ is a *waiting link*. It represents that member i waits from time k to time $k+1$ at location (l, z).
- Link $(l, z, k) \rightarrow^{r} (l', z', k') \in E^{ig}_{travel}$ is a *travel link*. It represents that member i travels on route r from location (l, z) to location (l', z') from time k to time k', where $k' - k$ is the travel time on route r.
- Link $(a, l, z, m, k) \rightarrow (a, l, z, m', k+1) \in E^{ig}_{exchange}$ is a *member-exchange link*. It represents that at a given location (l, z), if $m \subset m'$, a group of members $m' \setminus m$ joins m in performing activity a at time k; if $m \supset m'$, a group of members $m \setminus m'$ leaves m while performing activity a at time k; where $m' \setminus m$ is a group of members in m' but not in m, and both m, m' include i.
- Link $(l, z, k) \rightarrow (a, l, z, m, k+1) \in E^{ig}_{ingress}$ is an *activity-ingress link*. It means that a group of members m, including i, enters activity a at location (l, z) at time k.
- Link $(a, l, z, m, k) \rightarrow (l, z, k+1) \in E^{ig}_{egress}$ is an *activity-egress link*. It means that a group of members m, including i, leaves activity a at location (l, z) at time k.
- Link $Start(i) \rightarrow (l, z, 1) \in E^{ig}_{start}$ is a *start link*. It is a *dummy* start link for member i beginning his/her activity/travel plans at location (l, z).
- Link $(l, z, K+1) \rightarrow End(i) \in E^{ig}_{end}$ is an *end link*. It is a *dummy* end link for member i ending his/her activity/travel plans at location (l, z).

Fig. 1 illustrates the expansion of PJATS supernetworks G^{i1g} and G^{i2g} for two members $i1$ and $i2$ with a number of study time intervals $K = 4$. In this example, the pedestrian network has two locations, $loc1$ and $loc2$. Members $i1$ and $i2$ begin and end their activity/travel plans at $loc1$ and $loc2$, respectively. The two members have lunch on the 9th floor of $loc2$. With the proposed PJATS supernetwork, a path from node $Start(i)$ to

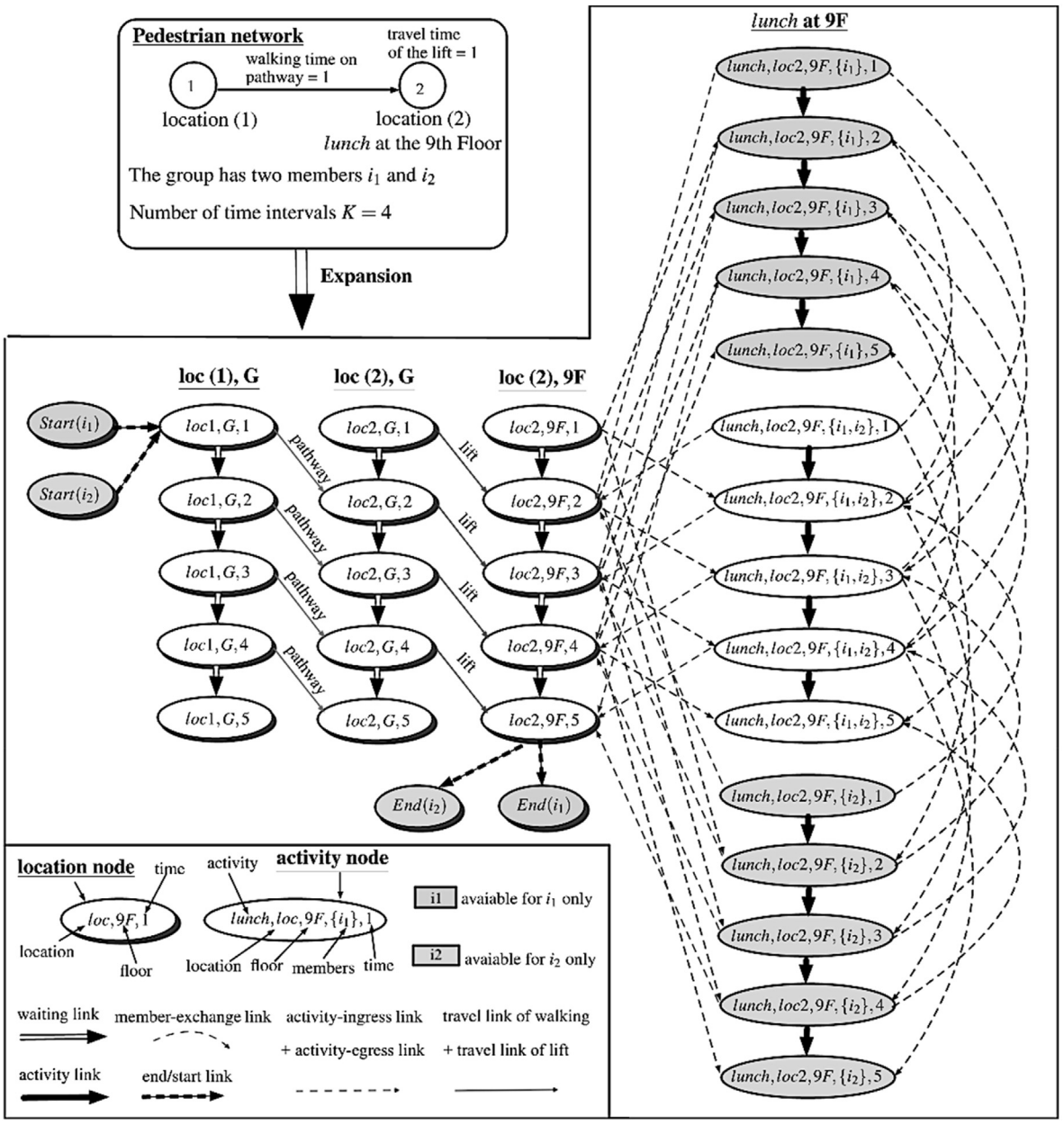

Fig. 1. PJATS supernetworks for two members $i1$ and $i2$.

node *End*(i) in supernetwork G^{ig} represents a *feasible activity-travel pattern* (ATP) of member i that takes into account joint activities between i and other members of group g. A *feasible joint activity-travel pattern* (JATP) of group g is composed of feasible ATPs of group members so that the spatiotemporal consistency in the joint activities of the ATPs involved is maintained.

3.2. Link utility/disutility in PJATS supernetwork

Let $u^0_{ia}(k)$ denote the utility gained when member i *separately* performs activity a at time k. The utility of member i performing activity a with the crowding discomfort effect at location (l, z) between times k and $k+1$, denoted by $u^i_a(k)$, can be expressed as

$$u^i_a\left(k\right) = \int_k^{k+1} u^0_{ia}\left(x\right) dx \left[1 - \alpha^i_a \left(f^z_l(k)/C^z_l\right)^{\theta^a_{lz}}\right] \tag{1}$$

where $\alpha^i_a \geq 0$ is the crowding discomfort sensitivity of member i to the crowdedness of activity a, $f^z_l(k)$ and C^z_l are the flow and capacity, respectively, at location (l, z) between times k and $k+1$, and θ^a_{lz} is the parameter related to the congestion effect of activity a at location (l, z).

The joint utility $u^g_a(k)$ gained when a group of members g jointly performs activity a between times k and $k+1$ is given by

$$u^g_a(k) = \sum_{i \in g} w^{ig}_a u^i_a(k) + \frac{\lambda_a}{2} \sum_{i,j \in g, i \neq j} w^{ig}_a u^i_a(k) w^{ig}_a u^i_a(k) \tag{2}$$

where $\lambda_a \geq 0$ is a parameter that represents the intragroup interactions for the joint participation of activity a, and w^{ig}_a is member i's weight parameter representing the relative influence of member i in group g on joint activity participation of activity a. A detailed interpretation of the group utility function and alternative formulations that represent various group decision-making strategies can be found in Zhang et al. (2009).

Let $v_r(k)$ denote the disutility for traveling on route r with departure

time k. The travel disutility is given by

$$v_r(k) = -VOT_r.t_r(k)\left[1+\beta_r\left(f_r(k)/C_r\right)^{\theta_r}\right] \quad (3)$$

where $VOT_r \geq 0$ is the value of time, $\beta_a \geq 0$ is the congestion discomfort parameter, $f_r(k)$ and C_r are the flow and capacity, respectively, between times k and $k + t_r(k)$, and θ_r is the parameter related to the congestion effect for traveling on route r. Note that the value of VOT_r is relative to the route. For example, the value of the time needed to walk on routes with steps or obstacles might be higher than that needed to walk along a corridor.

4. JATP scheduling model

In the JATP scheduling model, pedestrians in the same group schedule their activities and travels to maximize the group utility. With the PJATS supernetwork proposed in Section 3, the activity-travel scheduling decisions are equivalent to the determination of a path in the JPATS supernetwork for each group member such that the summation of the utilities of paths of all members is maximized while maintaining spatiotemporal consistency among the paths. The set of paths in the JPATS supernetwork that satisfy the above conditions then represents the optimal JATP.

4.1. Optimal JATP

Let P^{ig} denote the set of paths in supernetwork G^{ig} for member i of group g. The utility of path $p \in P^{ig}$, denoted as u_p^{ig}, can be obtained by the summation of the utilities of the links on path p as follows.

$$u_p^{ig} = \sum_{e \in E^{ig}} \psi_e^{ig} \delta_{ep}^{ig} \quad (4)$$

where $\delta_{ep}^{ig} = 1$ if path p contains link e and $\delta_{ep}^{ig} = 0$ otherwise, and ψ_e^{ig} is the utility of link e on path $p \in P^{ig}$. The utility ψ_e^{ig} is given by

- if $e \in E_{wait}^{ig} \cup E_{exchange}^{ig} \cup E_{ingress}^{ig} \cup E_{egress}^{ig} \cup E_{start}^{ig} \cup E_{end}^{ig}$, then $\psi_e^{ig} = 0$,
- if $e \in E_{act}^{ig}$ with $e = (a, l, z, m, k) \rightarrow (a, l, z, m, k+1)$, then $\psi_e^{ig} = u_a^m(k)$,
- if $e \in E_{travel}^{ig}$ with $e = (l, z, k) \rightarrow^r (l', z', k')$, then $\psi_e^{ig} = v_r(k)$,

where $u_a^m(k)$ and $v_r(k)$ are the activity utility and travel disutility given by Equations (2) and (3), respectively.

Let S^g denote the set of all feasible JATPs of group g, S^g can be defined with respect to ATPs of members i in group g, P^{ig}, in the following equation:

$$S^g = \left\{R \middle| !\nabla(p,p'), \forall p, p' \in R,\ R \in \times_{i \in g} P^{ig}\right\} \quad (5)$$

where R is a feasible JATP of group g, the term $\times_{i \in g} P^{ig}$ is the *cross product* of sets P^{ig}, and condition $\nabla(p,p')$ is true if path p conflicts with path p'. The condition $\nabla(p,p')$ is given by Definition 2, where e^{pk} denotes the link on path $p \in P^{ig}$ elapsed through time k to time $k+1$, and m^{pk} denotes the set of members related to link e^{pk}. Then, $m^{pk} = m \subseteq g$ when link e^{pk} takes one of the following forms:

- $e^{pk} = (a, l, z, m, k) \rightarrow (a, l, z, m, k+1) \in E_{act}^{ig}$,
- $e^{pk} = (l, z, k') \rightarrow^r (l', z', k'') \in E_{travel}^{ig}, k' \leq k \leq k''$,
- $e^{pk} = (a, l, z, m', k) \rightarrow (a, l, z, m'', k+1) \in E_{exchange}^{ig}, m' = m$ or $m'' = m$,
- $e^{pk} = (l, z, k) \rightarrow (a, l, z, m, k+1) \in E_{ingress}^{ig}$,
- $e^{pk} = (a, l, z, m, k) \rightarrow (l, z, k+1) \in E_{egress}^{ig}$.

Otherwise, $m^{pk} = \varnothing$.

Definition 1. (Link conflict). Given two links $e^{pk} \in E^{ig}$ and $e^{p'k} \in E^{i'g}$ with their corresponding sets of members m^{pk} and $m^{p'k}$, link e^{pk} conflicts with link $e^{p'k}$, denoted as $\nabla(e^{pk}, e^{p'k})$, if $m^{pk} \cap m^{p'k} \neq \varnothing$ and $e^{pk} \neq e^{p'k}$.

Definition 2. (Path conflict). Given two paths p and p', path p conflicts with path p', denoted by $\nabla(p, p')$, if $\exists k: \ \nabla(e^{pk}, e^{p'k}), k = 1...K$.

Let $\Phi^g \in S^g$ denote the feasible JATP of group g with greatest utility, or the optimal JATP of group g, where the JATP utility is the summation of utilities of ATPs of all group members. The optimal JATP of group g can be expressed as

$$\Phi^g = \underset{R \in S^g}{\operatorname{argmax}} \sum_{i \in g} \sum_{p \in R \cap P^{ig}} u_p^{ig}. \quad (6)$$

Note that $R \cap P^{ig}$ in Equation (6) represents a unit set for the feasible ATP p of member i in JATP R of group g such that p does not conflict with ATPs of other members of group g in terms of time and space.

4.2. JATP scheduling model formulation

Based on the proposed PJATS supernetwork, the JATP scheduling problem can be transformed into an extended static UE traffic assignment problem. This paper considers behaviorally heterogeneous classes of pedestrians and intragroup interactions of pedestrians in the same group. The JATP choices in the pedestrian network reach equilibrium if (1) pedestrians cannot improve their utility by unilaterally changing their ATPs to any other feasible ATPs, and (2) pedestrians in the same group must ensure the spatiotemporal consistency among their ATPs when they perform joint activities. In other words, the utilities of all used JATPs are the greatest, and all unused JATPs have smaller utilities. The UE condition can be expressed as

$$f_p^{ig}\left(\phi^{ig} - u_p^{ig}\right) = 0, \forall p \in R \cap P^{ig}, R \in S^g, g \in \Lambda, \quad (7)$$

$$\phi^{ig} - u_p^{ig} \geq 0, \forall p \in R \cap P^{ig}, R \in S^g, g \in \Lambda, \quad (8)$$

$$q^{ig} = \sum_{R \in S^g} \sum_{p \in R \cap P^{ig}} f_p^{ig}, \forall g \in \Lambda, \quad (9)$$

$$f_p^{ig} \geq 0, \forall p \in R \cap P^{ig}, R \in S^g, g \in \Lambda, \quad (10)$$

where

f_p^{ig}: the flow on path p related to the ATP of member i of group g,
ϕ^{ig}: the utility of optimal ATP of member i of group g,
q^{ig}: the demand for member i of group g,
Λ: the set of groups.

The flow on link e in the PJATS supernetwork can be determined by

$$x_e = \sum_{g \in \Lambda} \sum_{i \in g} \sum_{R \in S^g} \sum_{p \in R \cap P^{ig}} f_p^{ig} \delta_{ep}^{ig}. \quad (11)$$

Then, if $e \in E_{act}^{ig}$, x_e represents the crowdedness at the corresponding activity location in which member i of group g participates. If $e \in E_{travel}^{ig}$, x_e represents the traffic flow of the corresponding route on which member i of group g travels. The UE problem can then be expressed below as the minimization problem of the following gap function

$$\min GAP = \sum_{g \in \Lambda} \sum_{i \in g} \sum_{R \in S^g} \sum_{p \in R \cap P^{ig}} f_p^{ig}\left(\phi^{ig} - u_p^{ig}\right). \quad (12)$$

The UE solution convergence can be evaluated by the relative gap

(RGAP) (Fu and Lam (2014))

$$RGAP = GAP \Big/ \sum_{g\in\Lambda}\sum_{i\in g}\sum_{R\in S^g}\sum_{p\in R\cap P^{ig}} f_p^{ig} u_p^{ig}. \quad (13)$$

5. Heuristic solution method

In this section, an Algorithm for the MAPF problem to determine the optimal JATP is first presented. Based on this algorithm, a heuristic solution for the UE problem is proposed.

5.1. Solution algorithm to find the optimal JATP

The proposed PJATS supernetwork does not ensure spatiotemporal consistency among paths $p \in P^{ig}$ of members i in group g if each path for each member is searched separately in each G^{ig}. Therefore, the optimal JATP defined by Equation (6) is not simply the path with the greatest utility in each network G^{ig} separately. The path-finding problem must be treated as a MAPF problem in which each member is regarded as an agent, and the conflicts between member i and other members in the same group are considered simultaneously in the path-finding process for each G^{ig}. To solve the MAPF problem, we propose a solution Algorithm based on the conflict-based search (CBS) proposed by Sharon et al. (2015). The pseudo-code of the proposed solution algorithm is given below.

Algorithm. Conflict-Based Search

Inputs: $G^{ig}(N^{ig}, E^{ig})$, $\forall i \in g$;
Outputs: The optimal GATP Φ^g;
1. $C0 = \emptyset$;
2. $R0 = \{pi | i \in g\}$, where pi is the greatest-utility path in G^{ig} based on $C0 = \emptyset$;
3. $\Gamma = \{(R0, C0)\}$;
4. **while** $Q \neq \emptyset$ **do**
5. $(R, C) =$ the best element in Q, where R is the JATP with maximum utility;
6. $Q = Q \setminus \{(R, C)\}$;
7. **if** JATP R has no conflict **then**
8. **return** $\Phi^g = R$;
9. Determine a conflict between path $p \in R \cap P^{ig}$ and path $p' \in R \cap P^{i'g}$, $i \neq i'$, at time interval k' by Definition 1;
10. **for** each member i, i' involved in the conflict **do**
11. $RR = R$;
12. **if** member i avoids the conflict **then**
13. $CE = \{e^{pk}$ and all links of G^{ig} that conflict with link $e^{p'k}\}$;
14. $CC = C \cup CE$;
15. Replace $p \in RR \cap P^{ig}$ by the greatest-utility path in G^{ig} based on CC;
16. **else if** member i' avoids the conflict **then**
17. $CE = \{e^{p'k}$ and all links of $G^{i'g}$ that conflict with link $e^{pk}\}$;
18. $CC = C \cup CE$;
19. Replace $p' \in RR \cap P^{i'g}$ by the greatest-utility path in $G^{i'g}$ based on CC;
20. $Q = Q \cup \{(RR, CC)\}$;

The key idea of the above Algorithm is that the conflict is examined at each time k between path $p \in RR \cap P^{ig}$ and path $p' \in RR \cap P^{i'g}$, with $i \neq i'$ (Line 9). If there is a conflict, either member i or member i' avoids the conflict, that is, either path p uses link e^{pk} or path p' uses link $e^{p'k}$. The details for the development, optimality, and completeness of the CBS can be found in Sharon et al. (2015). The path-finding problem in each iteration of the CBS for each G^{ig} is a longest-path problem. The problem is known to be NP-hard for a general graph. Fortunately, the PJATS supernetwork G^{ig} constructed for each member i is a directed *acyclic* graph (see Fig. 1). Thus, paths with the greatest utility can be determined via dynamic programming.

5.2. Heuristic solution for extended UE problem

Based on the solution Algorithm for the optimal JATP proposed in Section 5.1, the extended UE problem can be solved without requirement of JATP enumeration. The solution algorithm for the extended UE problem is outlined as follows.

Step 1: Network expansion. Transform the pedestrian network into PJATS supernetworks $G^{ig}(N^{ig}, E^{ig})$, $\forall i \in g$, $g \in \Lambda$.
Step 2: **Initialization.** Let $n = 0$. Find the optimal JATP Φ^g using the CBS Algorithm in supernetworks $G^{ig}, \forall i \in g$, $g \in \Lambda$. Assign all demand q^{ig} on ATP p for member i in JATP Φ^g, i.e. $f_p^{ig(n)} = q^{ig}, \forall p \in \Phi^g, i \in g$, $g \in \Lambda$. Set $S^g = \{\Phi^g\}, \forall g \in \Lambda$. Update link flows and link utilities.
Step 3: **Column generation.** Find the optimal JATP Φ^g using the CBS Algorithm in supernetworks G^{ig}, $\forall i \in g$, $g \in \Lambda$. Update $S^g = S^g \cup \{\Phi^g\}, \forall g \in \Lambda$.
Step 4: **Flow update.** Find the optimal JATP Φ^g among JATPs in S^g. Assign all demand q^{ig} on ATP p for member i in JATP Φ^g to obtain the auxiliary flow for ATP p, i.e. $f_p^{ig(aux)} = q^{ig}, \forall p \in \Phi^g, i \in g$, $g \in \Lambda$. Set $f_p^{ig(aux)} = 0$ if ATP p for member i is not in JATP $\Phi^g, \forall p \notin \Phi^g, i \in g, g \in \Lambda$. Obtain the flow $f_p^{ig(n+1)}, \forall p \in R \cap P^{ig}$, $R \in S^g$, $i \in g$, $g \in \Lambda$, using MSA (method of successive averages) as below.

$$f_p^{ig(n+1)} = f_p^{ig(n)} + {}^1\!/_n \left(f_p^{ig(aux)} - f_p^{ig(n)}\right).$$

Then, update link flows and link utilities.

Step 5: **Convergence test.** For an acceptable convergence level ε, if RGAP $\leq \varepsilon$, **Stop.** Otherwise let $n = n + 1$ and go back to **Step 3.**

6. Numerical example

The numerical example aims to illustrate (1) the results of the proposed model and the convergence of the solution, (2) the sensitivity of the proposed model with respect to intragroup interaction, (3) the application of the proposed model to evaluate facility management policies, and (4) the possible use of Wi-Fi tracking data to generate activity patterns from the matched media access control (MAC) address of the detected pedestrians in a selected area within the PolyU campus.

6.1. Input data

In the numerical example, a simplified pedestrian network (as shown in Fig. 2) on the campus of PolyU is adapted to illustrate the essential ideas of the proposed supernetwork platform. The study network consists of six locations: locations (1) (student halls), (2) (canteen), (3) (entrance 1), and (5) (entrance 2) on the ground floor, and locations (4) and (6) (classrooms) on the ninth floor of the Block Z building (Faculty of Construction and Environment (FCE)). These six locations are related to three common activities of FCE students: home, study (lecture), and eating activities. Note that the study network covers only a small area of the PolyU campus at which MAC address scanners are installed for this case study. In addition, only students who lived in the student hall are considered, although some PolyU students may live off campus.

Pathways for walking are only available between locations on the same floor. There are two lifts (lifts 1 and 2) at entrances 1 and 2 on the ground floor, respectively, to provide access to the ninth floor. Parameters related to the travel disutility of link types (i.e., pathways or lifts) are presented in Table 1. The lift capacity is less than the pathway capacity and results in greater crowding discomfort.

The study horizon is the 9 h from 10:00 to 19:00. Each hour was divided into 60 equal intervals, that is, 1 min per interval. We assumed that all students begin and end their schedules at the student halls. Students can perform four types of activities: staying *home* in a student hall, *eating* and/or *café* at the canteen, and attending a *lecture* in the classroom. No congestion effect was considered when a student stays in a student hall or attends a *lecture* in the classroom. The capacity of the canteen was set to 300 students per minute. It was assumed that students perceive the utility functions of the four activities identically. The bell-shaped marginal utility function proposed by Ettema and Timmermans (2003) was adopted (see Fig. 3).

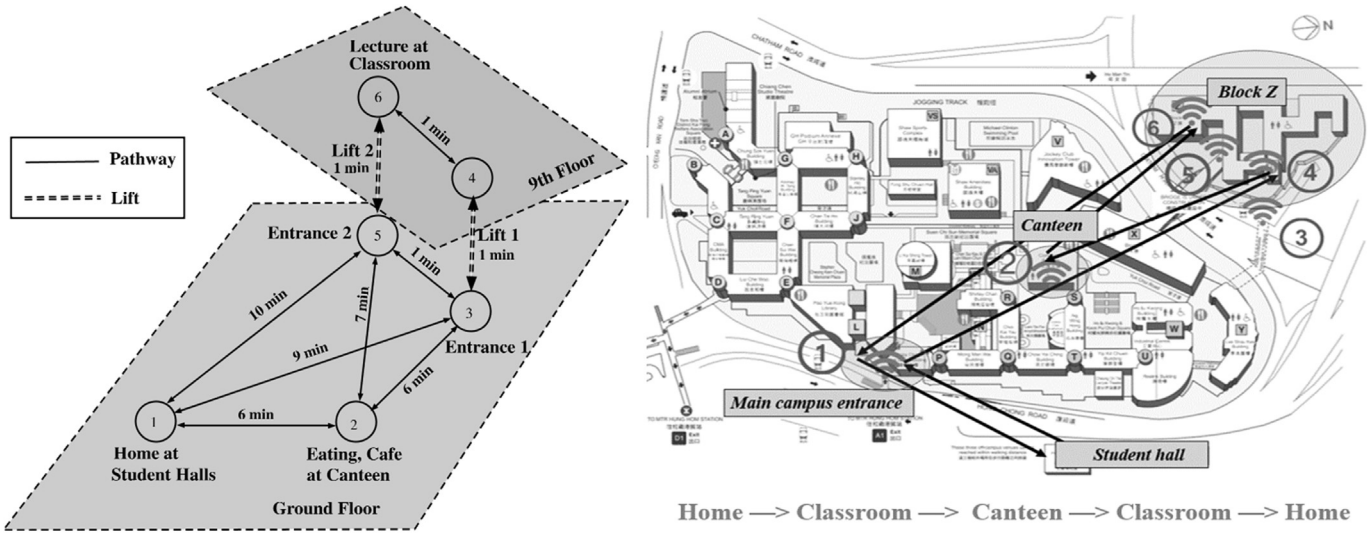

Fig. 2. Simplified pedestrian network on PolyU campus.

Table 1
Basic link data for the example pedestrian network.

Parameters	Link type	
	Pathway	Lift
Capacity C_r (students/minute)	70	6
Crowding discomfort parameters β_r, θ_r	30, 2	60, 4
Value of time VOT_r (HK$/minute)	1	1

The numerical example aims to illustrate JATPs to model the intragroup interactions of two behaviorally heterogeneous student classes: *A* and *B*. Table 2 shows all feasible group types for two student classes. To facilitate the presentation of essential ideas on the joint activity issue, it is assumed that class *A* students may only take part in joint activities with class *B* students. In other words, intragroup interactions between either two class *A* students or two class *B* students are ignored in this paper. Thus, there are only three group types, *X, Y,* and *Z,* as shown in Table 2. In particular, each group with type *X* (or *Y*) consists of only one student from class *A* (or *B*) who has no intragroup interactions with class *B* (or *A*) students. Each group with type *Z* comprises one student from class *A* and one from class *B* performing activities jointly. However, it should be noted that the proposed model is not restricted to scenarios with only two student classes and three possible group types. The extension of the proposed model is recommended for further studies with consideration of multiuser classes and various combinations of group types.

The total number of students was 500. For illustrative purposes, 250 class *A* students were assumed to have joint activities with 250 class *B* students. Thus, the demand for the JATPs of class *A* and *B* students with intragroup interactions was 250. Note that in reality, the numbers of class *A* and *B* students are not necessarily equal. For example, suppose that 300 class *A* students have joint activities with 200 class *B* students. In that case, the travel demand for class *A* and *B* students with intragroup interactions would be 200 each. The remaining 100 class *A* students would be considered separately without intragroup interactions.

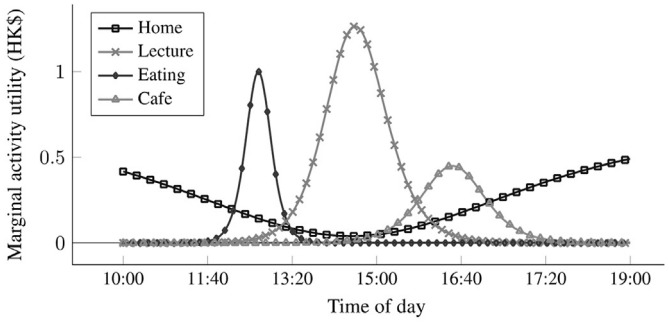

Fig. 3. Simplified temporal utility profiles of four activities.

The parameters related to student and group types for activity utility as shown in Equations (1) and (2) were set as $w_a^{AZ} = w_a^{BZ} = 0.5$, $w_a^{AX} = w_a^{BY} = 1$, $\lambda_a = 0.4$, $\alpha_a^A = 0.4$, $\alpha_a^B = 0.6$, and $\theta_{lz}^a = 2$, where activity a can be either eating or café. It must be noted that $\alpha_a^A = 0.4$ and $\alpha_a^B = 0.6$ mean that students in class *B* are more sensitive to crowding discomfort at the location of activity a than students in class *A*.

6.2. Numerical results

We considered the base case in which the number of groups with type *Z* is 125 over the population of 500 students. That means that the numbers of groups with types *X* and *Y* were each 125. The results are presented in Fig. 4 for the temporal distribution of students at activity locations and on travel links. Between 12:00 and 12:30, approximately 70% of students leave the student halls and go to the canteen for lunch by traveling on link 1–2. For the 13:30–15:30 period, all students are in the classroom because of the significant high utility of the lecture. From 15:20, students begin to leave the classroom and head to the café due to the lecture's decreasing utility. Due to the congestion at the canteen, approximately 50% of students go straight to the student halls without visiting the canteen for café. It can be observed from Fig. 4 that students do not arrive at and leave the classroom at the same time, but rather within certain periods, such as 12:45–13:45 and 15:20–16:20, before and after a lecture, respectively, because the only way to enter and leave the classroom is via lifts 1 and 2. However, because the lifts have a smaller capacity (i.e., six students per minute) than the 70 students per minute on the pathways, it takes some time for the lifts to carry all of the students.

The proposed solution Algorithm required about 55 min for 5000 iterations to solve the UE problem (Windows 10, Intel Core i5 3.50 GHz, 8 GB RAM). This computation time is acceptable for strategic planning purposes, although the study network is relatively small with six activity locations. Even with its small size, the study network still covers most commonly used activity-travel patterns of FCE students. If the study network was larger and included different student types from different faculties, the computation time would increase in a linear fashion with respect to the number of student types. This does not prevent the applicability of the proposed model in practice because the model is intended for long-term facility planning purposes for which the computation time is not the main concern.

Table 2
Feasible group types for intragroup interactions of two student classes.

			Student 1			
			Class A		Class B	
			With intragroup interactions	Without intragroup interactions	With intragroup interactions	Without intragroup interactions
Student 2	Class A	With intragroup interactions	✓	N.A.	√ (group *Z*)	N.A.
		Without intragroup interactions	N.A.	✓	N.A.	√ (groups *Y, X*)
	Class B	With intragroup interactions	√ (group *Z*)	N.A.	✓	✓
		Without intragroup interactions	N.A.	√ (groups *X, Y*)	✓	N.A.

√: feasible group type; N.A.: infeasible group type.

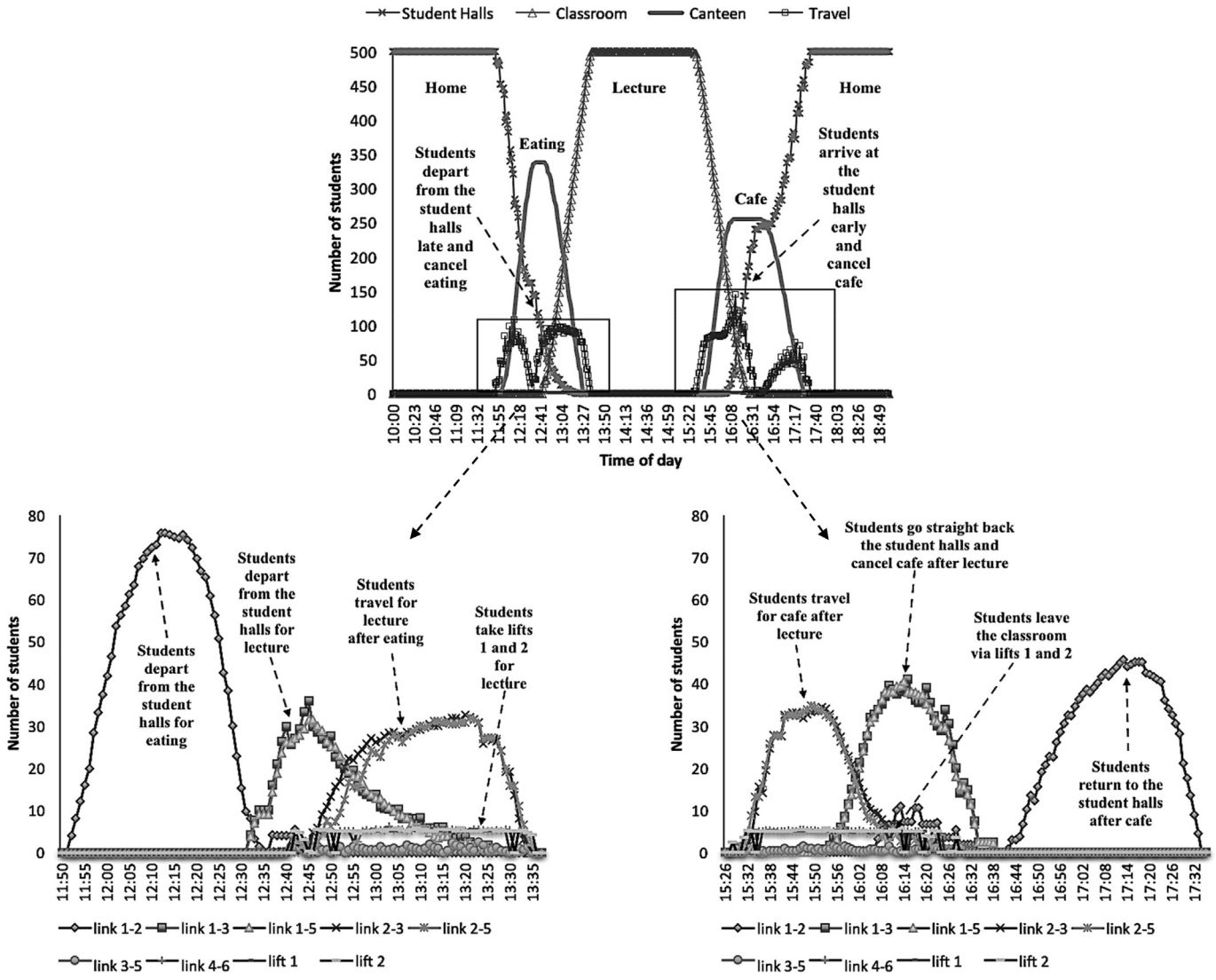

Fig. 4. Spatial student distribution at activity location and travel links.

Fig. 5 illustrates the convergence characteristics of the proposed heuristic solution method. The convergence pattern fluctuates significantly, and the MSA fails to converge, likely because the mapping function in Equation (4) is not strictly monotonic. However, the fluctuation seems stationary. We can interpret such regular fluctuation as day-to-day adjustment of the students' activity-travel behavior, in which each iteration step is regarded as the students' adjustment in making their activity-travel choices on a given day based on the information from previous days.

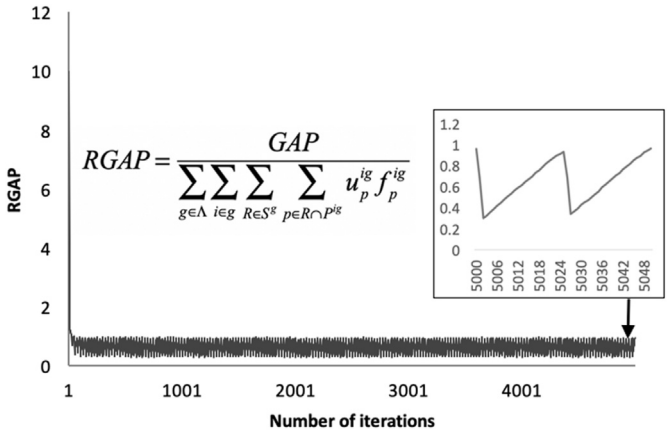

Fig. 5. Convergence characteristics of proposed UE heuristic solution method.

6.3. Sensitivity analysis of intragroup interactions

Let N_Z denote the number of groups with type Z. In other words, N_Z is the number of pairs of students who may perform joint eating and/or café. The sensitivity analysis results are given in Table 3. The sensitivity analysis of parameter N_Z shows that the travel demand for students' trip chains and the activity allocations not only depend on the individual activity utility, they also have a significant dependence on intragroup interactions among students.

As shown in Table 3, the increase in N_Z results in an increasing average duration of joint eating and café. In addition, class A students always spend more time on eating and café than class B students. These results can be explained by the higher utilities of joint eating and café and the smaller crowding discomfort sensitivity of class A. However, as N_Z decreases, the duration of eating and café for class B students increases, whereas class A students spend less time on eating and café, because when more students perform eating and café in pairs, a number of class A students, who perform activities separately, cancel eating and/or café or shorten the activity durations due to the crowding discomfort at the canteen.

6.4. Evaluation of facility management policies using the proposed model

In this section, the proposed model is used to evaluate facility management policies. We used the base case setting (i.e., $N_Z = 125$). Suppose that the university proposes two policies to evaluate the significance of lift 1 and the canteen. Specifically, Policy I is to close lift 1, and Policy II is to expand the canteen's capacity from 300 students per minute to 500 students per minute. Figs. 6 and 7 depict the effects of Policies I and II on population distributions at various activity locations. Table 4 lists the detailed results of the average activity time allocation with the effects of the two policies and their benefits of the policies shown in bold.

Fig. 6 shows that Policy I results in earlier departure times and later arrival times of students to and from the student halls. The durations of eating and café activities also increase. These outcomes result from the increase in the time required when only elevator 2 is used to carry all students and lift 1 is not operating. The students then tend to depart earlier and leave activity locations later to wait for the lift to be less congested. With Policy II, more students go to the canteen for eating and to the café for longer activity durations than the distribution in the base case given in Fig. 4. This is explained by the larger number of students who go to the canteen for eating and café and the increase in eating and café durations (see Fig. 7).

Table 3
Comparison of results by student classes of three scenarios.

Student class	$N_Z = 0$		$N_Z = 75$		$N_Z = 125$(*)	
	A	*B*	*A*	*B*	*A*	*B*
Travel demand of trip chains						
Home-Eating-Lecture-Home	7	73	69	5	105	11
Home-Lecture-Café-Home	0	0	0	0	15	18
Home-Eating-Lecture-Café-Home	203	0	181	73	128	95
Home-Lecture-Home	40	177	0	172	2	126
Average time allocation of activities (hours/student)						
Home (at the student halls)	4.41	5.29	4.24	5.06	4.37	4.76
Lecture (at the classroom)	2.56	3.16	2.63	2.85	2.65	2.85
Eating (at the canteen)	**0.83**	*0.15*	**0.82**	*0.26*	**0.81**	*0.36*
Café (at the canteen)	**0.98**	*0.00*	**0.85**	*0.42*	**0.70**	*0.59*
Average travel time (hours)	0.49	0.40	0.46	0.41	0.47	0.44
Total time (hours/student)	9.00	9.00	9.00	9.00	9.00	9.00

N_Z: number of groups with type Z, (*): the base case.

6.5. Using Wi-Fi tracking data to generate activity patterns of pedestrians

In this case study, the experiments were performed on the campus of PolyU. MAC addresses were collected from the six Wi-Fi scanners at various activity locations on campus (see Fig. 2). The locations chosen for the installed Wi-Fi scanners were the main entrance of the campus to capture students from the student halls, the student canteen, entrances, and classrooms at Block Z building for FCE. These places are major activity locations for FCE students. Because this experimental study was performed in the context of a university campus, it was expected that major activities (e.g., studying and eating) would be conducted at the selected locations. With that being said, the installed Wi-Fi scanners detected most students who entered and left the buildings concerned. Activity episodes were therefore extracted by matching the entering and leaving records from the same MAC address from the scanners within a feasible time window. Incomplete episodes, i.e., those with only a single detection, were then discarded. Although the Wi-Fi scanners could not capture all activity in the study area, the detected activities can still serve as samples to study the representative JATPs of university students.

Fig. 8 shows the flow chart for generation of pedestrians' activity patterns from Wi-Fi tracking data. There were three main steps, as illustrated. First, the raw Wi-Fi data were preprocessed via a set of filters to eliminate outliers and leave only the pedestrians' signatures. The Wi-Fi scanners were installed mainly at various entrance gates, and signatures were captured when pedestrians walked between activities. Second, *density-based spatial clustering of applications with noise* (DBSCAN) was applied to the records from each MAC address from various scanners to separate activities. This Algorithm was used to aggregate Wi-Fi

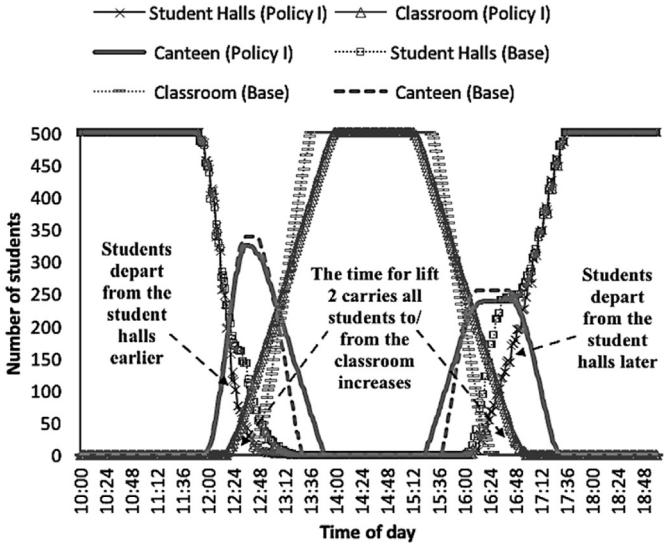

Fig. 6. Spatiotemporal student distribution with Policy I.

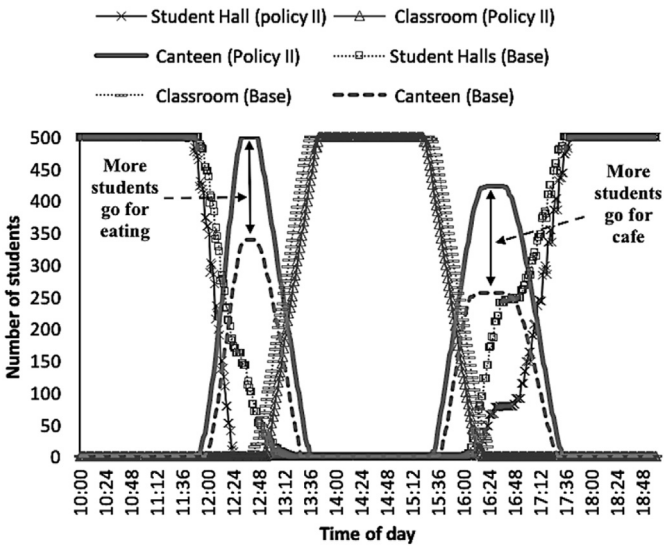

Fig. 7. Spatiotemporal student distribution with Policy II.

Table 4
Effects of Policies I and II on average time allocation of activities (hours/student).

	Home	Lecture	Eating	Café	Travel
Base case (1)	4.57	2.76	0.58	0.64	0.45
Policy I (2)	4.00	2.48	0.96	1.06	0.50
Policy II (3)	4.34	2.89	0.66	0.66	0.45
Difference (2)–(1)	*−0.57*	*−0.28*	**0.38**	**0.42**	*0.05*
Difference (3)–(1)	*−0.23*	*0.13*	**0.08**	**0.02**	*0*

signatures that belong to the same walking trip in a fast and unsupervised approach. Once different walking trips were separated, activity episodes were extracted from two consecutive walking trips. Finally, a hidden Markov model (HMM) was applied to all extracted activity episodes to identify similar activities in terms of the samples' spatial and temporal characteristics. The distribution of various activity patterns was determined by labeling the generated activity types from HMM back to individual temporally ordered activity episodes of all detected pedestrians.

Wi-Fi tracking data collected on Tuesday, September 4, 2018 are used for illustration in this example. There were 1433 pedestrians (unique MAC addresses) detected by the six Wi-Fi scanners on the survey day. The following sections show the detailed procedures and generated results for each step.

Step 1: Initial data processing

The initial processing aims to filter out vehicular devices (e.g., car dashcams) and fixed devices (e.g., printers) captured by Wi-Fi scanners because their existence will disturb the analysis of pedestrians' movement. Vehicular devices can be identified by their vendors and fixed devices by their frequency of detection. Devices captured continuously are most likely to be fixed devices near the detection region. After this noise is eliminated, the remaining pedestrian signatures are ready for activity analysis.

Step 2: Generation of activity episodes

DBSCAN is a density-based unsupervised clustering Algorithm that is often used to deal with large-scale spatial data. The details of this algorithm can be found in Ester et al. (1996). In this example, DBSCAN is used to separate Wi-Fi signatures from different trips for each pedestrian. Because the study area is a university campus and most of the transfers can be finished within 15 min, the maximum distance between two signatures in one cluster is set to be finished in 15 min. The minimum number of signatures required to form a cluster is set to be one for each trip, which must be captured by at least one scanner. In this way, each resulting cluster represents one walking trip between two activities. The activity episode information can be extracted from two consecutive walking trips. To be specific, the earliest timestamp in one walking trip's signatures is the end time of the first activity, and the latest timestamp is the start time of the second activity. When a group of pedestrians conducts one joint activity, activity episodes that have a start time and end time with small differences at the same Wi-Fi scanner (activity location) will be generated by different group members. JATPs can then be generated by identifying these activity episodes at each Wi-Fi scanner.

Fig. 9 summarizes the results of Step 2. The left-hand figure shows the distribution of activity episodes from all detected pedestrians. Most pedestrians (88.76%) have one to three activity episodes, and the maximum number of episodes recorded for a pedestrian is five. The figure on the right-hand side illustrates the distribution of group members participating in activities. Most activities are solo (95.53%), and most group activities include two persons. The biggest group has six pedestrians. Fig. 10 illustrates the detected activity patterns of two pedestrians and their joint activities.

Step 3: Activity pattern generating

Having extracted activity episodes from Wi-Fi data, it is possible to identify similar activity types to analyze pedestrians' JATPs at an aggregate level. HMM is adopted here to label detected activities into groups with similar spatiotemporal characteristics. HMM is a time-state model that can discover the hidden states from observed data in an unsupervised approach. Details of the formulations and solution algorithms about this method can be found in Rabiner (1989). In this example, the

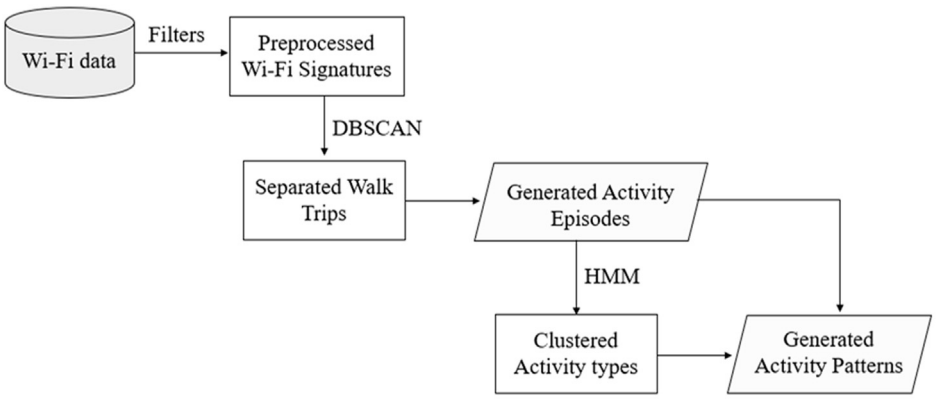

Fig. 8. Flowchart for generation of pedestrians' activity patterns from Wi-Fi tracking data.

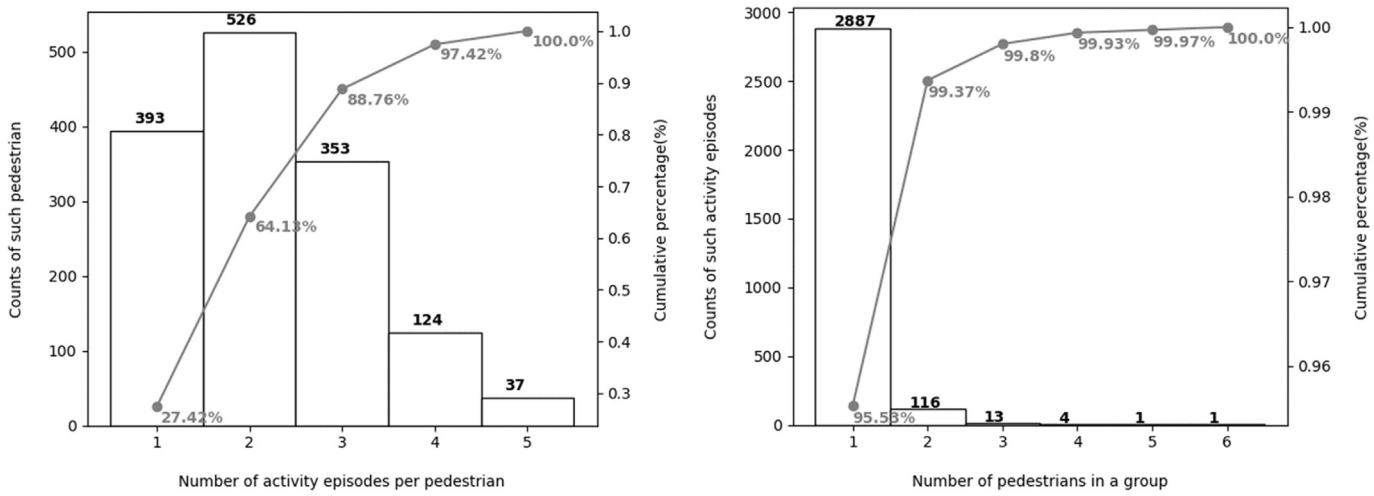

Fig. 9. Distribution of generated activity episodes and group activities. (left: distribution of activity episodes; right: distribution of group numbers).

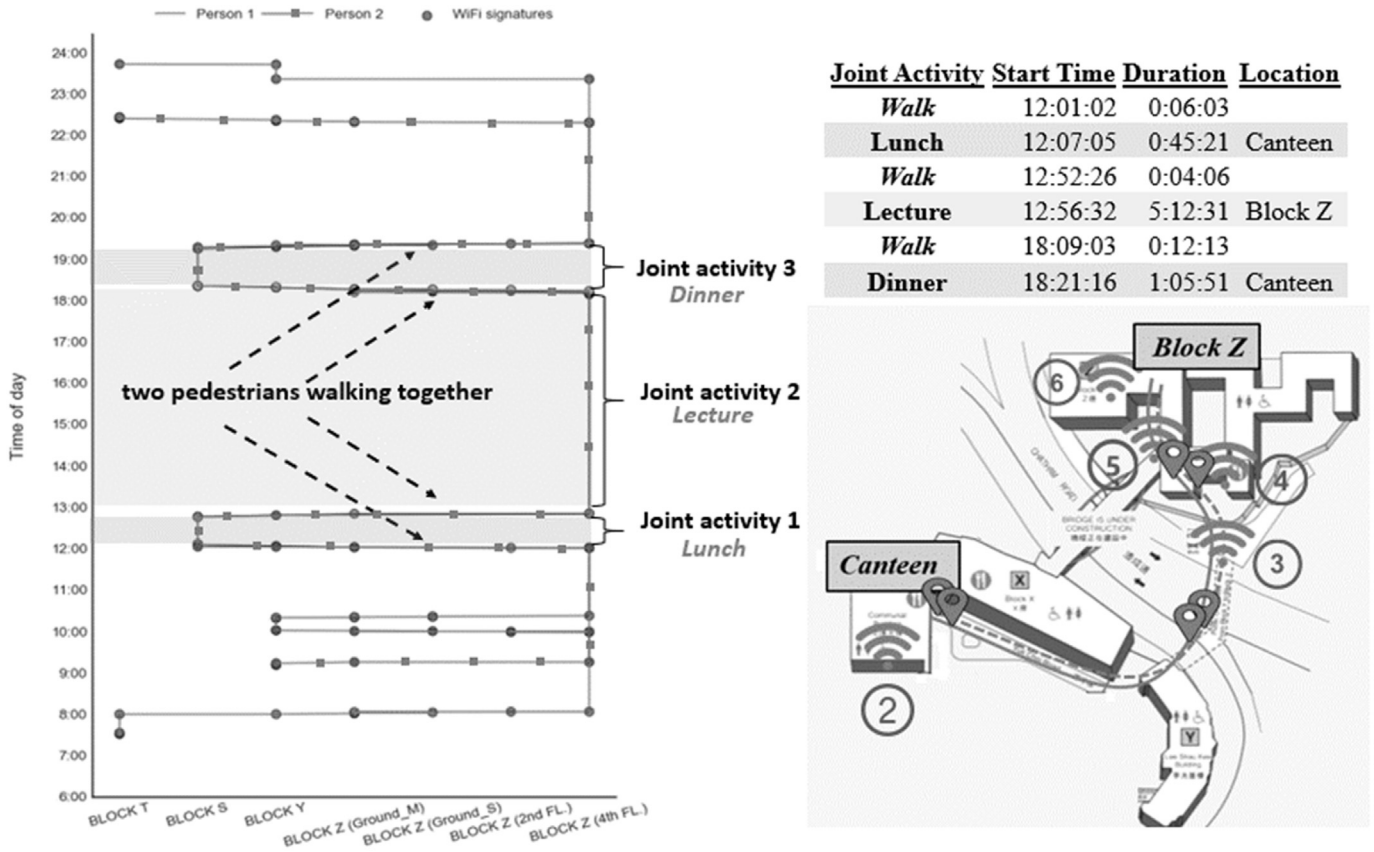

Joint Activity	Start Time	Duration	Location
Walk	12:01:02	0:06:03	
Lunch	12:07:05	0:45:21	Canteen
Walk	12:52:26	0:04:06	
Lecture	12:56:32	5:12:31	Block Z
Walk	18:09:03	0:12:13	
Dinner	18:21:16	1:05:51	Canteen

Fig. 10. Illustration of detected activity patterns of two pedestrians and their joint activities.

start time, duration, and location of all detected activity episodes from 1433 MAC addresses are the observed inputs in the HMM. The generated hidden states are referred to as various types of activities.

In reality, detailed in-campus activity types can be tedious to enumerate. To simplify the illustration and to be consistent with the proposed model results, the activity episodes detected by scanners are all aggregated into two general categories: studying and eating. To further demonstrate the captured characteristics of these two activity types, Fig. 11 shows the joint distribution of the start time and duration for studying activities and eating activities. Studying activity occurs on campus throughout the day in three major clusters, denoted S1, S2, and S3 for later analysis. Eating activity occurs in two distinct clusters, denoted E1 and E2.

By labeling each individual's temporally ordered activity episodes with the generated activity types, the distribution of various activity patterns is shown in Table 5. It can be observed that 38 activity patterns can be extracted from 1433 pedestrians' Wi-Fi signatures. On average, each pedestrian has 2.2 activities captured by Wi-Fi scanners. Frequently observed patterns include two daytime studying activities (S1–S2), two daytime studying activities separated by one eating activity (S1-E1-S2) (15.91%), one morning studying activity (S1) (12.42%), and one afternoon studying activity (S2) (11.24%). In addition, some unique (or

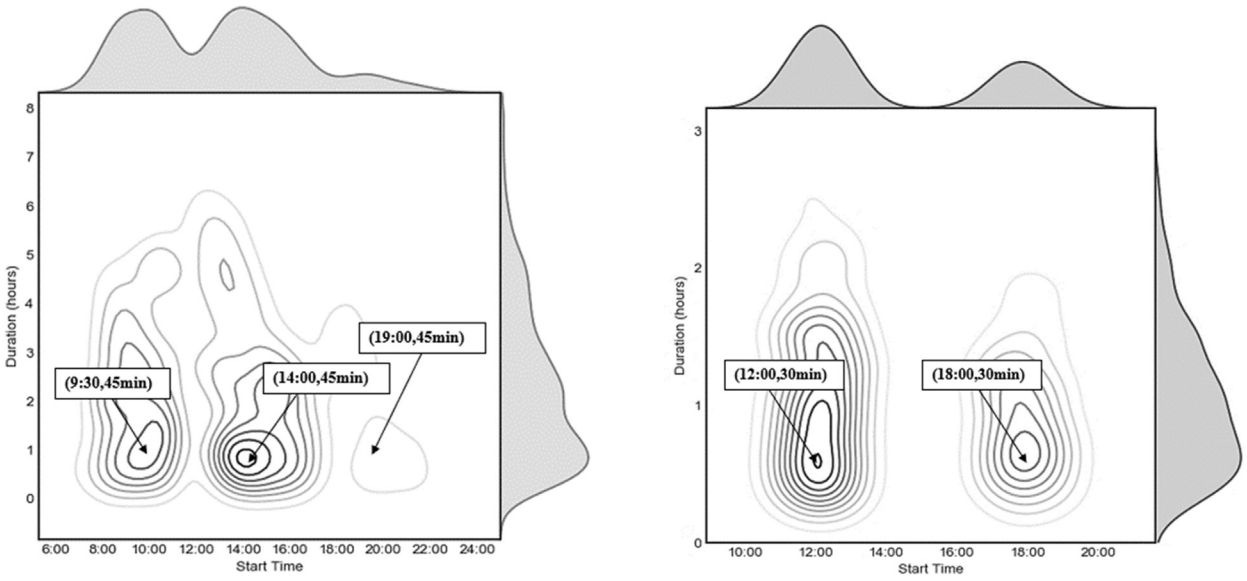

Fig. 11. Joint distribution plot of duration and start time per activity type. (left: studying activity; right: eating activity).

Table 5
Distribution of activity patterns from detected pedestrians.

No.	Pattern	Count	Percentage	No.	Pattern	Count	Percentage
1	**S1–S2**	228	**15.91%**	20	E1-S2-E2-S3	11	0.77%
2	**S1-E1-S2**	227	**15.84%**	21	S1-E2	10	0.70%
3	**S1**	178	**12.42%**	22	S1-E1-S1	10	0.70%
4	**S2**	161	**11.24%**	23	E1	9	0.63%
5	E1-S2	96	6.70%	24	S1-E2-S3	9	0.63%
6	S1-E1	80	5.58%	25	S2-E2-S2	4	0.28%
7	S1-E1-S2-E2	74	5.16%	26	S1-E1-S1-S2	4	0.28%
8	S2-E2	63	4.40%	27	S1-E1-S2-E2-S2	4	0.28%
9	S1–S2-E2	46	3.21%	28	E1-S1-S2	3	0.21%
10	S1-E1-S2-E2-S3	32	2.23%	29	E1-S2-S3	3	0.21%
11	S3	29	2.02%	30	S1–S2-E2-S2	3	0.21%
12	E2-S3	26	1.81%	31	E2-S2	2	0.14%
13	S2–S3	18	1.26%	32	S1–S3	2	0.14%
14	E1-S2-E2	17	1.19%	33	S2-E1-S2	2	0.14%
15	E2	16	1.12%	34	S1-E2-S2	2	0.14%
16	S2-E2-S3	16	1.12%	35	S1-E1-S1-E2	2	0.14%
17	S1-E1-S2-S3	16	1.12%	36	E1-S1	1	0.07%
18	S1–S2–S3	14	0.98%	37	E1-S2-E2-S2	1	0.07%
19	S1–S2-E2-S3	13	0.91%	38	S1-E1-S1-E2-S3	1	0.07%
					Total	***1433***	***100%***

S1: studying activities that started between 06:00 and 12:00 with the peak occurrences at 9:30.
S2: studying activities that started between 12:00 and 18:00 with the peak occurrences at 14:00.
S3: studying activities that started between 18:00 and 23:00 with the peak occurrences at 19:00.
E1: eating activities that started between 8:00 and 15:00 with the peak occurrences at 12:00.
E2: eating activities that started between 15:00 and 20:00 with the peak occurrences at 18:00.

abnormal) activity patterns come from fewer than 10 pedestrians (see pattern numbers 23–38 in Table 5). The uniqueness may be a result of abnormal activity time choices or unusual combinations of activity episodes. These unique patterns are indeed meaningful even though they were chosen by a small number of students. Note that whether a pattern is abnormal or not depends on the proportion of detected pedestrians (1433 persons) in the actual population under study. However, further grouping of these unique patterns can be considered for further analysis as needed.

7. Conclusions

This paper proposed a new activity-based equilibrium model to schedule the JATPs of pedestrians with use of Wi-Fi data. The multilayer structure of pedestrian networks and the joint activities of pedestrians were captured by a PJATS supernetwork platform. A heuristic solution based on CBS and MSA was proposed to solve the JATP scheduling problem. A simplified pedestrian network in the study area within the university campus of PolyU was used to show the application of the proposed model for facility planning and management purposes. The results of the numerical example show that the proposed model could reasonably reproduce the JATPs of students in various scenarios. It was also demonstrated that the Wi-Fi data collected in the study area of the PolyU campus could be used to generate the daily activity pattern of pedestrians and their joint activities from the MAC addresses of the detected pedestrians.

To calibrate and validate the proposed model, more than 30 Wi-Fi scanners were recently installed around the campus to investigate the

activity-travel patterns of pedestrians with use of Wi-Fi data. About 100 students will be hired to carry out a travel diary survey by activating the Wi-Fi connection on their communication devices (with the MAC address recorded) while they are on campus during selected weekdays. The generated activity patterns will then be validated by a paper-based travel diary survey completed by the hired/invited students. The experiment will be repeated for different groups of students (e.g., different departments, full-time/part-time students) to ensure that a variety of data are collected in terms of different activities, locations, and schedules by time of day.

It is worth mentioning that the given experimental study by Wi-Fi tracking benefited from the reliable campus wireless network and the high penetration of Wi-Fi-enabled devices among university students. When this approach is used in another context in a different environment, the performance of the proposed approach may be affected by the valid samples based on the matched Wi-Fi data only. As we enter the 5G era, multiple types of sensors and fully connected infrastructure will be available in the near future. Therefore, future studies should extend the proposed model with the use of multiple sources of urban big data for smart city development.

Declaration of competing interest

The authors declare that they have no known competing financial interests or personal relationships that could have appeared to influence the work reported in this paper.

Acknowledgments

The research in this paper was jointly supported by research grants from the Research Grants Council of the Hong Kong Special Administrative Region (Project No. PolyU 152057/15E) and The Hong Kong Polytechnic University (Project No. 1-ZVFJ).

References

Arentze, T., Timmermans, H., 2004. Multistate supernetwork approach to modelling multi-activity, multi-modal trip chains. Int. J. Geogr. Inf. Sci. 18 (7), 631–651.

Bhat, C., Guo, J., Srinivasan, S., Sivakumar, A., 2004. Comprehensive econometric microsimulator for daily activity-travel patterns, Transportation Research Record. J. Transport. Res. Board 1894 (1), 57–66.

Bierlaire, M., Robin, T., 2009. Pedestrians choices. In: Timmermans, H. (Ed.), Pedestrian Behavior. Emerald Group Publishing Limited, pp. 1–26.

Ester, M., Kriegel, H.P., Sander, J., Xu, X., 1996. A density-based Algorithm for discovering clusters in large spatial databases with noise. In: Proceedings of the Second International Conference on Knowledge Discovery and Data Mining (KDD-96), pp. 226–231.

Ettema, D., Timmermans, H., 2003. Modeling departure time choice in the context of activity scheduling behavior, Transportation Research Record. J. Transport. Res. Board 1831 (1), 39–46.

Fu, X., Lam, W.H.K., Meng, Q., 2014. Modelling impacts of adverse weather conditions on activity travel pattern scheduling in multi-modal transit networks. Transportmetrica B 2 (2), 151–167.

Fu, X., Lam, W.H.K., 2014. A network equilibrium approach for modelling activity-travel pattern scheduling problems in multi-modal transit networks with uncertainty. Transportation 41 (1), 37–55.

Fu, X., Lam, W.H.K., 2018. Modelling joint activity-travel pattern scheduling problem in multi-modal transit networks. Transportation 45 (1), 23–49.

Hoogendoorn, S., Bovy, P., Daamen, W., 2002. Microscopic Pedestrian Way Finding and Dynamics Modelling. Pedestrian and Evacuation Dynamics. Springer, Berlin, pp. 123–155.

Hoogendoorn, S., Bovy, P., 2004. Pedestrian route-choice and activity scheduling theory and models. Transport. Res. Part B 38 (2), 169–190.

Lam, W.H.K., Yin, Y., 2001. An activity-based time-dependent traffic assignment model. Transport. Res. Part B 35 (6), 549–574.

Li, Z.C., Lam, W.H.K., Wong, S.C., Sumalee, A., 2010. An activity-based approach for scheduling multimodal transit services. Transportation 37 (5), 751–774.

Miller, E., Roorda, M., 2003. Prototype model of household activity-travel scheduling, Transportation Research Record. J. Transport. Res. Board 1831 (1), 114–121.

Ouyang, L.Q., Lam, W.H.K., Li, Z.C., Huang, D., 2011. Network user equilibrium model for scheduling daily activity travel patterns in congested networks, Transportation Research Record. J. Transport. Res. Board 2254 (1), 131–139.

Rabiner, L., 1989. A tutorial on hidden Markov models and selected applications in speech recognition. Proc. IEEE 77 (2), 257–286.

Roorda, M.J., Carrasco, J.A., Miller, E.J., 2009. An integrated model of vehicle transactions, activity scheduling and mode choice. Transport. Res. Part B 43 (2), 217–229.

Sharon, G., Stern, R., Felner, A., Sturtevant, N.R., 2015. Conflict-based search for optimal multi-agent path finding. Artif. Intell. 219, 40–66.

Vo, K.D., Lam, W.H.K., Chen, A., Shao, H., 2020. A household optimum utility approach for modeling joint activity-travel choices in congested road networks. Transport. Res. Part B 134, 93–125.

Zhang, J., Kuwano, M., Lee, B., Fujiwara, A., 2009. Modeling household discrete choice behavior incorporating heterogeneous group decision-making mechanisms. Transport. Res. Part B 43 (2), 230–250.